Diffusion Rates for Hydrogen on Pd(111) from Molecular Quantum Dynamics Calculations

ARTICLE *in* JOURNAL OF PHYSICAL CHEMISTRY LETTERS · NOVEMBER 2014

Impact Factor: 7.46 · DOI: 10.1021/jz502251w

4 AUTHORS, INCLUDING:

Thiago Diamond Reis Firmino
Université Paris-Sud 11
8 PUBLICATIONS **2** CITATIONS
SEE PROFILE

Fabien Gatti
Institut Charles Gerhardt
137 PUBLICATIONS **2,171** CITATIONS
SEE PROFILE

W. Dong
Ecole normale supérieure de Lyon
22 PUBLICATIONS **48** CITATIONS
SEE PROFILE

THE JOURNAL OF PHYSICAL CHEMISTRY Letters

Letter

pubs.acs.org/JPCL

Diffusion Rates for Hydrogen on Pd(111) from Molecular Quantum Dynamics Calculations

Thiago Firmino,[†,§] Roberto Marquardt,[*,†] Fabien Gatti,[‡] and Wei Dong[¶]

[†]Laboratoire de Chimie Quantique, Institut de Chimie, UMR 7177 CNRS/Université de Strasbourg, 1 rue Blaise Pascal, BP 296/R8, 67008 Strasbourg Cedex, France

[‡]CTMM, Institut Charles Gerhardt, UMR 5253 CNRS/Université de Montpellier 2, 34095 Montpellier Cedex 05, France

[¶]Laboratoire de Chimie, UMR 5182 CNRS/Ecole Normale Supérieure de Lyon, 46 Allée d'Italie, 69364 Lyon Cedex 07, France

Supporting Information

ABSTRACT: The van Hove formula for the dynamical structure factor (DSF) related to particle scattering at mobile adsorbates is extended to include the relaxation of the adsorbates' vibrational states. The total rate obtained from the DSF is assumed to be the sum of a diffusion and a relaxation rate. A simple kinetic model to support this assumption is presented. To illustrate its potential applicability, the formula is evaluated using wave functions, energies, and lifetimes of vibrational states obtained for H/Pd(111) from first-principle calculations. Results show that quantum effects can be expected to be important even at room temperature.

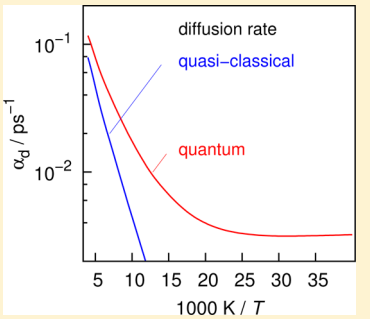

SECTION: Surfaces, Interfaces, Porous Materials, and Catalysis

The diffusion of adsorbed particles is of fundamental importance to a number of physical and chemical processes on surfaces, including film or crystal growth, the formation of nanostructures on surfaces, associative desorption, chemical reactions, and heterogeneous catalysis.[1] This elementary process has been explored in quasi-elastic helium atom scattering experiments,[2] among other techniques. With improved energy resolution, in ^{3}He spin−echo experiments,[3−6] diffusion time scales became accessible. The primary result from these experiments is the intermediate scattering function (ISF) $I(\boldsymbol{q},t)$, where $\boldsymbol{q}$ is the wave vector related to the momentum transferred from the scattered atoms to the adsorbed particles moving on the surface and t is the time. The ISF is the spatial Fourier transform of the pair correlation function proposed by van Hove.[7]

In the experimental work, the diffusion rate of the adsorbed particles is obtained either from adjustments of time-dependent model exponential functions to the ISF or from the determination of an effective energy broadening of the dynamical structure factor (DSF) $S(\boldsymbol{q},E)$ after deconvolution with an experimental response function. The DSF is the temporal Fourier transform of the ISF. In ref 7, van Hove also derived a general expression for the DSF in terms of the eigenvalues and eigenfunctions pertaining to the stationary states of the adsorbates.

In the present work, a simple extension of van Hove's formula for the DSF is proposed that allows us to deduce the diffusion rate from the full width at half-maximum (fwhm) of the DSF. The new formula involves the energies and wave functions of stationary states of the nuclear motion of the adsorbates and, in addition, their lifetimes. Our rather simple theoretical framework is capable of yielding a comprehensive assessment of the DSF from ab initio calculations. It can hence be evaluated to yield diffusion rates using nonadjustable parameters, which has so far not been achieved. Also, as will be explained below, it implies that the total width of the DSF should be interpreted as the sum of two terms, a relaxation term, related to the finite lifetime of vibrational states, and a diffusion term. This interpretation is new and may potentially lead to a novel method to exploit experimentally obtained diffusion rates in order to deduce vibrational lifetimes from them.

Previous quantum mechanical treatments of diffusion rates range from a quantum transition-state theory,[8] transition-state wave packet[9] and path integral methods,[4,10,11] polaron-like theories for tunneling diffusion,[12,13] or a Monte Carlo wave function formalism.[14] All of these treatments rely either on adjustable parameters or on approximations. In refs 11−14, relaxation of the adsorbate's motion due to couplings with surface electrons or phonons has been considered. Classical[15−18] and quantum[19] molecular dynamics calculations were performed to elucidate the form of the DSF and to infer the role of friction and experimental resolution on the resulting quasi-elastic broadening. In ref 19, a damped harmonic oscillator model was used, and parameters were adjusted to describe the line shape of vibrations parallel to the substrate. To

Received: October 24, 2014
Accepted: November 25, 2014

   dx.doi.org/10.1021/jz502251w | J. Phys. Chem. Lett. XXXX, XXX, XXX−XXX

our knowledge, there is so far no quantum theoretical treatment of diffusion rates relying on first-principle calculations of the DSF itself. Also in this respect, our method is innovative as it should enable us to validate ab initio calculations from a comparison with experimental data, and vice versa, without the need to refer to adjustable parameters. Furthermore, by assessing the full DSF, our method allows us to describe the general motion of the adsorbates and not only the dynamical behavior in the long time and space scale, which is related to diffusion.

In the present work, we extend van Hove's formulation of the DSF as follows

$$S(\boldsymbol{q}, E) = \sum_n P_n \sum_m \left| \sum_k^N \langle m|e^{i\boldsymbol{q}\boldsymbol{x}_k}|n\rangle \right|^2 L(E; (E_m - E_n), \Gamma_{nm}) \quad (1)$$

In this equation, $|n\rangle$ and $|m\rangle$ are multidimensional eigenstates of the nuclear motion of scattering centers on adiabatic potentials at energies E_n and E_m; P_n is the Boltzmann population distribution; $\boldsymbol{x}_k$ is the position vector of the adsorbed particle k (k = 1, ..., N). $L(E;E_0,\Gamma)$ is a normalized Lorentzian distribution peaked at E_0 and having a fwhm Γ. In the original work of van Hove, this formula is given with a δ function instead of the Lorentzian; the δ- function is a limiting case of the Lorentzian at $\Gamma \to 0$. Extending van Hove's original formula in this way is reasonable as $|n\rangle$ and $|m\rangle$ are not true eigenstates of the system; rather, they are coupled to the surrounding electrons or lattice vibrations (phonons). The coupling to a dense medium can be included in the dynamical treatment by replacement of the real eigenvalue for an otherwise stationary state $|n\rangle$ with a complex eigenvalue. If the imaginary part of the nth eigenvalue is written as $\gamma_n/4$, the population lifetime of state n is given by $\tau_n = h/(\pi\gamma_n)$, where h is the Planck constant. The Fourier transform of the time-dependent scattering function yields then a Lorentzian distribution rather than a δ function. In eq 1, $\Gamma_{nm} = (1/2)(\gamma_n + \gamma_m)$, which is the overall width (fwhm) arising from the combination of states $|n\rangle$ and $|m\rangle$. Equation 1 is derived in the Supporting Information.

In a recent work (unpublished results), we explored the prospect of eq 1 to calculate diffusion rates of adsorbates for simple model systems and adjustable parameters. In the present work, we go one step further by evaluating eq 1 using nonadjustable parameters. Eigenvalues and eigenfunctions are derived from a potential energy surface (PES) for the H/Pd(111) system.[20] Realistic values for the lifetimes of these states were calculated in ref 21. Both the PES and lifetimes have been derived from ab initio calculations. The availability of these data explains our choice of this system, for which experimental diffusion rates have not yet been determined, however.

While eigenstates of the nuclear motion can be calculated rather straightforwardly, if a global PES is known, the determination of their lifetimes is more involved, and data are scarce. Depopulation of vibrational eigenstates of adsorbates on metal substrates via formation of electron−hole pairs is expected to proceed on the picosecond time scale[22,23] or even faster.[21,24] This is about the time scale that can be reached with the ^{3}He spin−echo technique. Lifetimes for the lowest excited vibrational states in the most stable H/Pd(111) adsorption sites have been calculated to be around 500 fs to 1.5 ps.[21] The corresponding energy broadening range of 2.6−0.9 meV is up to 3 orders of magnitude larger than the broadening due to the diffusion of the adsorbates typically observed in the aforementioned ^{3}He spin−echo experiments. The relaxation rate due to the coupling to phonons is probably much smaller.[25]

For converged numerical evaluations of eq 1, sums over many states are needed, typically 50−200. As we do not know the lifetimes for the entire set of states, we make an ad hoc model assumption that consists of taking two different averaged lifetimes based on the results from ref 21; vibrational ground states, that is, node-less states at the stable adsorption sites, are supposed to have a lifetime longer than 1 μs, that is, a width of 1 neV, while all vibrationally excited states have an intrinsic lifetime of about τ_i = 527 fs, which corresponds to an intrinsic energy broadening $\gamma_i = h/(\pi\tau_i)$ = 2.5 meV.

We use the Multi-Configuration Time Dependent Hartree (MCTDH) program suite[26,27] to calculate eigenstates of the nuclear motion of the adsorbed particles. For technical details and how the analytical function derived in ref 20 was used, we refer to the Supporting Information. A graphical representation of a section of the PES is shown in Figure 1, which also shows

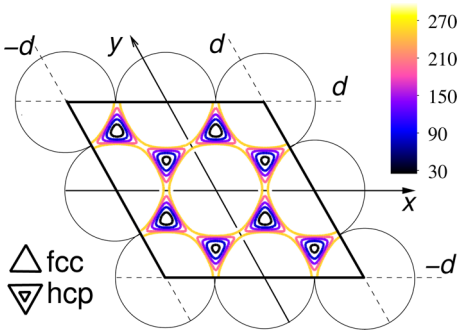

Figure 1. Scheme of the (2 × 2) surface cell used to characterize the H/Pd(111) system. x and y are skewed coordinates used in the dynamics. Palladium atoms are indicated by the large spheres of diameter d (d = 275.114 pm is the Pd−Pd bulk distance on the PES from ref 20). A section of the PES for atomic hydrogen at 90 pm above the substrate is superimposed on the scheme. Color-coded contour lines are given in units of meV.

the (2 × 2) surface cell underlying the present calculations. The stable adsorption sites denoted as "fcc" and "hcp" are clearly indicated. On this PES, the hcp site is about 25 meV less stable than the fcc site, and the barrier between the two sites is approximately 145 meV above the fcc site. There are four fcc and four hcp sites per unit cell. The present study mimics a coverage degree of 25%. Subsurface absorption sites are considerably higher in energy[28] and dynamically irrelevant in the present study for temperatures up to 400 K.

Each site has a local C_{3v} symmetry, such that per site, two vibrational modes parallel to the substrate and one mode perpendicular to it can be expected. The eight lowest eigenstates are node-less at a given site; four have significant probability densities at the fcc and four at the hcp sites. They describe vibrational ground states. Correspondingly, per site, there are 12 vibrationally excited states, namely, 8 states of parallel modes and 4 states of perpendicular modes, all arranged in levels of quasi-isoenergetic states. The eigenstates of nuclear motion can hence be cast into a coarse-grained level structure. Coarse-grained levels are identified by the vibrational quantum number related to a specific adsorption site, while nearly

dx.doi.org/10.1021/jz502251w | J. Phys. Chem. Lett. XXXX, XXX, XXX−XXX

degenerate states within a level compose a dense structure of eigenstates that are highly delocalized throughout the surface cell and that represent diffusion. Vibrations are highly anharmonic. In the low-energy domain, tunneling splits these levels; the ground-state tunneling levels at both the fcc and hcp sites span a range of about 0.6 μ eV, and these levels remain thus essentially degenerate. The vibrationally excited levels split into two blocks for each type of mode; the splitting varies between 60 and 500 μ eV for the parallel modes and reaches 1.3 meV for the perpendicular modes. These splittings could in principle be observed by high-resolution spectroscopy. Table 1 reports these splittings and summarizes expected transitions, assuming that they occur vertically on top of each adsorption site.

Table 1. Energies of the Fundamental Transitions for H/Pd(111) in meV

		theory			exp[29]
modes	site	this work		ref28	
parallel	fcc	92.19 (5)	92.25 (3)	88.94	96.0
	hcp	90.11 (3)	90.60 (5)		
perpendicular	fcc	129.88 (1)	131.24 (3)	114.36	126.0
	hcp	124.00 (3)	125.32 (1)		

Remaining degeneracies of transitions reported in Table 1 are indicated by the numbers in parentheses. The present results for vibrational transitions are comparable to recently reported theoretical values from ref 28 and agree fairly well with experimental data. In refs 28 and 29, only one value is reported per transition. In ref 10, larger transition energies and tunneling splittings were reported.

As a consequence of the coarse-grained level structure described above, the DSF can be decomposed into a sum $S(\boldsymbol{q},E) = \sum_l S_l(\boldsymbol{q},E)$, where $l = 1, 2, \ldots$ denotes a set of vibrational levels.

Evaluation of eq 1 with the eigenvalues and widths discussed above yields a very narrowly peaked function at $E = 0$, the width of which is 1 neV and corresponds to the average lifetime assumed in this work for the vibrational ground states. It depends only very feebly on $\boldsymbol{q}$. Note that as the Lorentzians in eq 1 are energy-normalized, the form of the DSF at $E \approx 0$ is dominated by the contributions from the level of ground states. It is reasonable to omit these contributions as they apparently do not influence the DSF further; in particular, they do not lead to any diffusion broadening. In the following, we consider therefore the differential DSF

$$\Delta S(\boldsymbol{q}, E) = S(\boldsymbol{q}, E) - S_1(\boldsymbol{q}, E) \quad (2)$$

where $S_1(\boldsymbol{q},E) \approx S_1(0,E)$ is the contribution to $S(\boldsymbol{q},E)$ from the level of the ground states. Figure 2 shows the normalized function $\Delta S(\boldsymbol{q},E)/\Delta S(\boldsymbol{q},0)$ along the $\langle 1\ 1\ \bar{2}\ 0\rangle$ direction for $T = 250$ K.

At first sight, the fwhm of this function again depends little on the transferred momentum wavenumber q. It is roughly given by $\Gamma_i = 2.5$ meV, as expected for the average intrinsic energy width adopted in the present work for the excited vibrational states. The DSF is not symmetrical. This is expected because in eq 1 the Boltzmann weight P_n stands for just one of the two vibrational levels $|n\rangle$ and $|m\rangle$ that are combined in the Lorentzian distribution. In particular, the features seen at 17 and 22 meV are due to combinations in eq 1 of states at the fcc

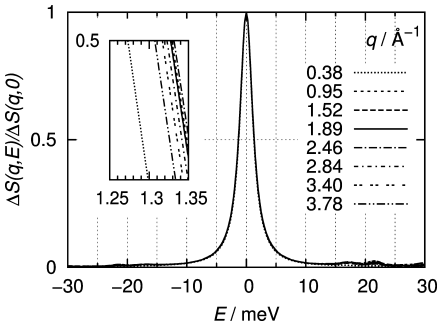

Figure 2. $\Delta S(\boldsymbol{q},E)/\Delta S(\boldsymbol{q},0)$ as a function of E and $\boldsymbol{q}$ for atomic hydrogen on Pd(111) at $T = 250$ K. The inset is a magnification of the function (right wing). Lines are cubic spline interpolations. $\langle 1\ 1\ \bar{2}\ 0\rangle$ crystallographic direction.

and hcp sites that have each one quantum of parallel vibration. Other features arising at higher energies are due to combinations of states having different vibrational quanta. The effect from these combinations on the quasi-elastic broadening is eliminated, when a high-energy filter is used in eq 1. In particular, a filter at 68 meV is used in the present calculations, which corresponds to a cutoff energy at the energy difference between a vibrationally excited state at the fcc site and a vibrational ground state at the hcp site. The overall shape of the DSF is thus nearly that of a Lorentzian, which corresponds to the expected shape in the strong damping limit.[17]

When the graph in Figure 2 is magnified, one sees, however, a neat progression of lines (inset in that figure). Clearly, it is the differential width $\Delta\Gamma = \Gamma - \Gamma_i$ that varies with $\boldsymbol{q}$. To show this variation in detail, we plot in Figure 3 the rate

$$\alpha_d = \frac{\pi\Delta\Gamma}{h} \quad (3)$$

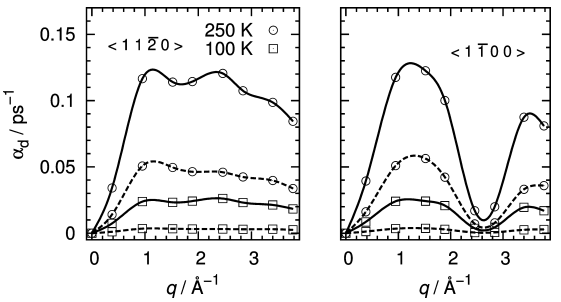

Figure 3. Diffusion rate (see the text) along two crystallographic directions and two temperatures, as indicated. Lines are cubic spline interpolations. The dashed lines yield the contribution from an "over-the-barrier" motion (see the text).

$\approx 0.759634\ \text{ps}^{-1} \times \Delta\Gamma/\text{meV}$. The solid lines in the figure give α_d. The solid line on the left-hand side, at 250 K, was obtained from the series of $\Delta S(\boldsymbol{q},E) = 0.5 \times \Delta S(\boldsymbol{q},0)$ intersections seen in the inset of Figure 2.

The dashed lines are obtained from the sole contribution of those states to the differential DSF, whose energies lie above the lowest possible effective hopping barrier between the fcc and hcp sites along the $\langle 1\ \bar{1}\ 0\ 0\rangle$ direction. This barrier, of about 104 meV, is obtained when the variation between the anharmonic zero-point energies at the barrier site (142 meV) and the fcc site (183 meV) are added to the aforementioned

dx.doi.org/10.1021/jz502251w | J. Phys. Chem. Lett. XXXX, XXX, XXX−XXX

electronic barrier of 145 meV. States contributing to such an "over-the-barrier" motion are hence all states excluding the vibrational ground level and the levels pertaining to the parallel modes in Table 1. The dashed lines give thus an idea of the contribution to the diffusion rate from over-the-barrier hops. For instance, at q = 0.95 Å^{-1} in the $\langle 1\ 1\ \bar{2}\ 0\rangle$ direction, the portion of over-the-barrier motion is 44% at 250 K, while it decreases to 15% at 100 K. Because of the inclusion of zero-point energy differences in the definition of the effective hopping barrier, the over-the-barrier motion should be considered as a quasi-classical description of the diffusion dynamics. Because the difference between the total diffusion rate and the over-the-barrier one is the pure contribution of tunneling, the latter provides an original means to see the contribution stemming from the tunneling effect.

This figure shows that α_d captures all qualitative features of diffusion rates observed experimentally in the quasi-elastic atom scattering experiments for other systems that are usually reported as functions of the momentum transfer q in the given crystallographic directions.[2−4] We note in particular the quadratic increase with q at $q \approx 0$ and the partially oscillatory behavior for larger values of q, which is typically related to jump diffusion. As an additional support for our interpretation of α_d as being the diffusion rate determined in the ^{3}He spin−echo experiments, Figure 4 shows an Arrhenius plot of the temperature dependence of α_d.

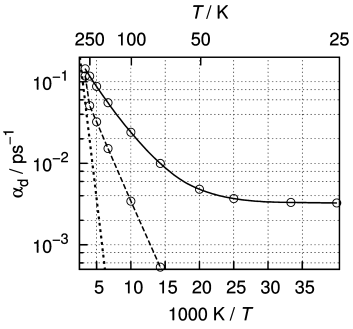

Figure 4. Arrhenius plot of the temperature dependence of α_d; $\langle 1\ \bar{1}\ 0\ 0\rangle$ crystallographic direction and q = 0.95 Å^{-1} (solid line). The dashed line is an estimate of the contribution from over-the-barrier motion, and the dotted line is from a classical Vineyard treatment (see the text).

We note first the qualitative change of the function at about 70 K, which clearly marks the crossover to the quantum tunneling regime evoked in previous theoretical work on similar systems.[4,13] In the high-temperature regime, we note second that the rates are at least 1 order of magnitude larger than those reported in ref 10 for the same system. This could be related to a somewhat stiffer potential used in that work. In order to shed more light onto potential "quantum effects" on the diffusion rate, we draw with a dashed line the diffusion rates obtained from over-the-barrier motion (see Figure 3 and the text above). The first five points on this line between 250 and 70 K can be nicely fit by a straight line yielding a different effective diffusion barrier of about 40 meV and a frequency factor of 0.30 ps^{-1}. The dotted line shows the result from a classical Vineyard-like rate estimate,[30] whose frequency factor of 15 ps^{-1} and barrier energy of 145 meV were determined from the present PES. Both the Vineyard-like rate and the over-the-barrier rate follow an Arrhenius law in the aforementioned temperature range. The latter has a flatter slope, which might be related to the use of a reduced hopping barrier of 104 meV via the inclusion of zero-point energy differences. Yet, this barrier is still a factor of 2 larger than the effective barrier determined from a fit to the Arrhenius law. A more detailed analysis of this behavior is out of the scope of the present work. However, even without further analysis, by comparing the solid line in Figure 4 with the dotted and the dashed lines, we illustrate the importance of quantum effects and the inability of simple activation theories to account for these effects at temperatures near to and below 300 K.

Third, in the low-temperature regime, the diffusion rate becomes nearly constant, which is in qualitative agreement with previous experimental[4] and theoretical[13] findings for similar systems. Equation 1 is in principle valid for all temperature ranges where Boltzmann statistics hold. In the high-temperature domain, a large number of states is needed to ensure convergence of the summation. The states considered in the present work allow us to converge calculations up to 300 K. The aforementioned filtering out of contributions from vibrational transitions to the quasi-elastic broadening is valid up to this temperature. In the low-temperature domain, it is known that a temperature-dependent renormalization of effective tunneling matrix elements may account for a small variation of the diffusion rate.[13] This effect is not implicitly included in the present treatment.

A simple kinetic model allows us to rationalize the variability of the differential width as a function of the transferred momentum. Starting from the kinetic model for jump diffusion,[31] we extend it to include relaxation by friction. We write the equation of motion for the probability of finding a particle at position $\boldsymbol{x}$ at time t as[18]

$$\frac{\partial P(\boldsymbol{x}, t)}{\partial t} = \frac{1}{\tau}\left(\sum_k \left(P(\boldsymbol{x} + y_k, t) - P(\boldsymbol{x}, t)\right)\right) - \frac{1}{\tau_i} P(\boldsymbol{x}, t) \quad (4)$$

The first part of the right-hand side involves summation over lattice vectors and corresponds to the original jump diffusion model; it leads to the well-known classical exponential decay for the ISF, if one assumes that the $P(\boldsymbol{x},t)$ equals $G_s(\boldsymbol{x},t)$, the self-part of the pair correlation function. This decay can be a more involved model expression of several exponential functions,[18] or it can be replaced by an even more complicated function that one might determine from quantum dynamics. The second part on the right-hand side of eq 4 leads to a simple exponential decay of the ISF. Now, the first part leads to a quasi-exponential decay; the total decay rate is hence given as the sum of the decay rates of the two parts. Consequently, it is the difference of the total width and the width due to relaxation by friction that depends strongly on the momentum transfer and that is generally related to the diffusion motion.

Relevant lifetimes from ref 21 differ only little from the generic average value adopted in the present work. Our result should be close to the result that one would obtain if lifetimes of individual vibrational states were used. It might be necessary though to include explicitly all of the individual lifetimes to arrive at a quantitative agreement with experiment, and we plan to do this work as well as to extend it to the study of higher substrate coverage degrees in the near future.

In the present Letter, an original theoretical framework is presented that allows us to assess diffusion rates of adsorbed particles in a parameter-free way using vibrational frequencies

dx.doi.org/10.1021/jz502251w | J. Phys. Chem. Lett. XXXX, XXX, XXX−XXX

and wave functions, as well as vibrational lifetimes obtained entirely from quantum mechanical ab initio calculations. The results obtained here for the H/Pd(111) system show important quantum effects that traditional semiempirical methods fail to reproduce. Our approach captures qualitatively properties of the diffusion rate observed for similar systems. The theory can be further refined by inclusion of lifetimes for individual states, and then, full quantitative reproduction of experimental data can be expected. The approach is based on a new interpretation of the measured widths of the DSF as the sum of a relaxation and diffusion broadening.

■ ASSOCIATED CONTENT

Ⓢ Supporting Information

A derivation of eq 1 as well as technical details of the calculations such as MCTDH specific settings. This material is available free of charge via the Internet at http://pubs.acs.org.

■ AUTHOR INFORMATION

Corresponding Author

*E-mail: roberto.marquardt@unistra.fr.

Present Address

[§]T.F.: Laboratoire de Chimie Physique d'Orsay, UMR 8000 CNRS/Université de Paris-Sud, 91405 Orsay Cedex, France.

Notes

The authors declare no competing financial interest.

■ ACKNOWLEDGMENTS

This work was carried out within a research program from the Agence Nationale de la Recherche (Project ANR 2010 BLAN 720). We thank ANR for the generous financial support, as well as CNRS and the Université de Strasbourg.

■ REFERENCES

(1) Barth, J. Transport of Adsorbates at Metal Surfaces: From Thermal Migration to Hot Precursors. *Surf. Sci. Rep.* **2000**, *40*, 75−149.

(2) Graham, A. P.; Menzel, A.; Toennies, J. P. Quasielastic Helium Atom Scattering Measurements of Microscopic Diffusional Dynamics of H and D on the Pt(111) Surface. *J. Chem. Phys.* **1999**, *111*, 1676−1685.

(3) Jardine, A. P.; Lee, E. Y. M.; Ward, D. J.; Alexandrowicz, G.; Hedgeland, H.; Allison, W.; Ellis, J.; Pollak, E. Determination of the Quantum Contribution to the Activated Motion of Hydrogen on a Metal Surface: H/Pt(111). *Phys. Rev. Lett.* **2010**, *105*, 136101.

(4) McIntosh, E. M.; Wikfeldt, K. T.; Ellis, J.; Michaelides, A.; Allison, W. Quantum Effects in the Diffusion of Hydrogen on Ru(0001). *J. Phys. Chem. Lett.* **2013**, *4*, 1565−1569.

(5) Jardine, A. P.; Hedgeland, H.; Alexandrowicz, G.; Allison, W.; Ellis, J. ^{3}He Spin Echo: Principles and Application to Dynamics at Surfaces. *Prog. Surf. Sci.* **2009**, *84*, 323−379.

(6) Jardine, A. P.; Alexandrowicz, G.; Hedgeland, H.; Allison, W.; Ellis, J. Studying the Microscopic Nature of Diffusion with Helium-3 Spin-Echo. *Phys. Chem. Chem. Phys.* **2009**, *11*, 3355−3374.

(7) van Hove, L. Correlations in Space and Time and Born Approximation Scattering in Systems of Interacting Particles. *Phys. Rev.* **1954**, *95*, 249−262.

(8) Wolynes, P. G. Quantum Theory of Activated Events in Condensed Phases. *Phys. Rev. Lett.* **1981**, *47*, 968−971.

(9) Zhang, D. H.; Light, J. C.; Lee, S.-Y. Transition State Wave Packet Study of Hydrogen Diffusion on Cu(100) Surface. *J. Chem. Phys.* **1999**, *111*, 5741−5753.

(10) Rick, S. W.; Lynch, D. L.; Doll, J. D. The Quantum Dynamics of Hydrogen and Deuterium on the Pd(111) Surface: A Path Integral Transition State Theory Study. *J. Chem. Phys.* **1993**, *99*, 8183−8193.

(11) Chen, L. Y.; Ying, S. C. Theory of Surface Diffusion: Crossover from Classical to Quantum Regime. *Phys. Rev. Lett.* **1994**, *73*, 700−703.

(12) Zhu, X. D. Conduction-Electron Effect in Quantum Tunneling Diffusion of Hydrogen on Metal Surfaces. *Phys. Rev. B* **1994**, *50*, 11279−11282.

(13) Sundell, P. G.; Wahnström, G. Quantum Motion of Hydrogen on Cu(001) using First-Principles Calculations. *Phys. Rev. B* **2004**, *70*, 081403.

(14) Badescu, S. C.; Ying, S. C.; Ala-Nissila, T. Quantum Diffusion of H/Ni(111) through a Monte Carlo Wave Function Formalism. *Phys. Rev. Lett.* **2001**, *86*, 5092−5095.

(15) Guantes, R.; Vega, J. L.; Miret-Artés, S.; Pollak, E. Kramers' Turnover Theory for Diffusion of Na Atoms on a Cu(001) Surface Measured by He Scattering. *J. Chem. Phys.* **2003**, *119*, 2780−2791.

(16) Jardine, A. P.; Ellis, J.; Allison, W. Effects of Resolution and Friction in the Interpretation of QHAS Measurements. *J. Chem. Phys.* **2004**, *120*, 8724−8733.

(17) Vega, J. L.; Guantes, R.; Miret-Artés, S. Quasielastic and Low Vibrational Lineshapes in Atom−Surface Diffusion. *J. Phys.: Condens. Matter* **2004**, *16*, S2879−S2894.

(18) Tuddenham, F. E.; Hedgeland, H.; Jardine, A. P.; Lechner, B. A.; Hinch, B.; Allison, W. Lineshapes in Quasi-Elastic Scattering from Species Hopping between Non-Equivalent Surface Sites. *Surf. Sci.* **2010**, *604*, 1459−1475.

(19) Vega, J. L.; Guantes, R.; Miret-Artés, S.; Micha, D. A. Collisional Line Shapes for Low Frequency Vibrations of Adsorbates on a Metal Surface. *J. Chem. Phys.* **2004**, *121*, 8580−8588.

(20) Xiao, Y.; Dong, W.; Busnengo, H. F. Reactive Force-Field for Surface Chemical Reactions: A Case Study with Hydrogen Dissociation on Pd Surfaces. *J. Chem. Phys.* **2010**, *132*, 014704.

(21) Tremblay, J. C. A Unifying Model for Non-Adiabatic Coupling at Metallic Surfaces beyond the Local Harmonic Approximation: From Vibrational Relaxation to Scanning Tunneling Microscopy. *J. Chem. Phys.* **2013**, *138*, 244106.

(22) Morin, M.; Levinos, N. J.; Harris, A. L. Vibrational Energy Transfer of CO/Cu(100): Nonadiabatic Vibration/Electron Coupling. *J. Chem. Phys.* **1992**, *96*, 3950−3956.

(23) Frischkorn, C.; Wolf, M. Femtochemistry at Metal Surfaces: Nonadiabatic Reaction Dynamics. *Chem. Rev.* **2006**, *106*, 4206−4233.

(24) Vazhappilly, T.; Beyvers, S.; Klamroth, T.; Luppi, M.; Saalfrank, P. Vibrationally Enhanced Associative Photodesorption of Molecular Hydrogen from Ru(0001). *Chem. Phys.* **2007**, *338*, 299−311.

(25) Head-Gordon, M.; Tully, J. C. Vibrational Relaxation on Metal Surfaces: Molecular-Orbital Theory and Application to CO/Cu(100). *J. Chem. Phys.* **1992**, *96*, 3939−3949.

(26) Beck, M. H.; Jäckle, A.; Worth, G. A.; Meyer, H.-D. The Multiconfiguration Time-Dependent Hartree (MCTDH) Method: A Highly Efficient Algorithm for Propagating Wavepackets. *Phys. Rep.* **2000**, *324*, 1−105.

(27) Meyer, H.-D.; Gatti, F.; Worth, G. A. *Multidimensional Quantum Dynamics*; Wiley-VCH: Weinheim, Germany, 2009.

(28) Tremblay, J. C.; Saalfrank, P. Selective Subsurface Absorption of Hydrogen in Palladium Using Laser Distillation. *J. Chem. Phys.* **2009**, *131*, 084716.

(29) Conrad, H.; Kordesch, M.; Scala, R.; Stenzel, W. Surface Resonances on Pd(111)/H Observed with HREELS. *J. Electron Spectrosc. Relat. Phenom.* **1986**, *38*, 289−298.

(30) Vineyard, G. H. Frequency Factors and Isotope Effects in Solid State Rate Processes. *J. Phys. Chem. Solids* **1957**, *3*, 121−127.

(31) Chudley, C. T.; Elliot, R. J. Neutron Scattering from a Liquid on a Jump Diffusion Model. *Proc. Phys. Soc.* **1961**, *77*, 353−361.